TRADE OFFS IN LQ/LTR CONTROL DESIGNS FOR MIMO AMB SYSTEMS

Rafał P. Jastrzębski

Dept. of Electrical Eng., Lappeenranta Univ. of Technology, Lappeenranta 53851 Finland
rjastrz@lut.fi

Riku Pöllänen

Dept. of Electrical Eng., Lappeenranta Univ. of Technology, Lappeenranta 53851 Finland
riku.pollanen@lut.fi

ABSTRACT

This study evaluates the design tradeoffs of linear-quadratic (LQ) and LQ / loop transfer recovery (LTR) controllers for MIMO AMB system. The comparison of the LQ regulator with the Kalman filter, LQ/LTR design, and classical PID and PI/PD cascaded controllers is presented.

The properties of the tested control configurations are examined using maximum singular values of the output sensitivity function of the close-loop system and the tolerated disturbance force at the input of the plant. Furthermore, the indexes such as measured peak output sensitivity, responses to the step reference position and step disturbance are examined. The simulation and experimental results from the test-rig are compared.

INTRODUCTION

In the control of AMBs the most widely used control methods utilize relatively straightforward controllers, for example, lead compensator with low-pass filter and cascaded PI/PD structure. However, the performance of these decentralized (local) controllers, which consider the rotor as two masses located at bearings, is limited by the simple control structures. The more sophisticated controllers, like model-based centralized (global) controllers may account for flexible modes of the rotor, known disturbances, and rotational speed dependent dynamics of the system. Therefore, they could provide better performance, but their drawbacks are the timely control design, complex implementation, and greater computational effort.

In recent years, new approaches in centralized as well as decentralized control of AMBs have been presented in the literature. A decentralized PI/PD position control of AMBs was examined in [1]. A multi-objective genetic algorithm was proposed as an optimization tool for designing decentralized AMB controllers in [2]. Schroder et al. [3] applied this approach in an on-line tuning of the AMB controller. In [2] and [3], the decentralized controller structure was based on the PI, lead compensator, and notch filter. A linear-quadratic (LQ) control with a switching controller (copper losses were optimal) was presented by Zhuravlyov in [4]. The LQ control based on the flexible rotor model obtained using finite element modeling (FEM) was studied in [5].

Finding an optimal AMB control structure and control design method, suitable for selected application, is not a trivial task. A credible comparison between various control strategies is difficult because of different tuning approaches. The manual selection of tuning parameters for different control methods yields, in fact, trial and error tuning.

This paper demonstrates a practical approach to the off-line tuning of the AMB model-based controllers. The work demonstrates a convenient method to automate the optimal tuning of the selected controller structures using the same objective function. This way, a credible comparison between the controllers of different structures is achieved. The proposed control design tuning method utilizes a genetic algorithm that efficiently contributes to the overall performance improvement over the best manually tuned reference designs.

The trade offs in the design of MIMO AMB control, with respect to the tolerated disturbance forces, and effectiveness of the feedback are highlighted. The obtained controllers are evaluated by simulations and experiments using the AMB test-rig. The work focuses on the radial suspension.

In the utilized test-rig a rotor alone weighted 46.2 kg. Two radial and one axial bearing were keeping the

rotor in suspension. In current controlled actuators we applied reduced premagnetization current equal to 0.25 times the maximum coil current. All the tested controllers were implemented using FPGA-PC-dSPACE™ prototyping control platform for rapid AMB control software development [5].

CONTROL DESIGNS

The classical decoupled PID control or its modifications, for example, cascaded PI/PD control are simple and in many applications sufficient control methods. Because of their popularity such a direct output feedback controllers are used here as references for comparison with more complex state-feedback, model-based controllers.

PID based control

For the decentralized control we apply the approach presented in [1] resulting in a PID like controller, with an additional first-order filter (or a lead compensator with an integrator). We use the controller with the transfer function

$$G_{ld}(s) = G_{P,ld}\left(\frac{\tau_{ld}s+1}{a_{ld}\tau_{ld}s+1} + \frac{a_I}{s\tau_I}\right), \quad (1)$$

$$\tau_{ld} = \frac{1}{\sqrt{a_{ld}}\omega_{ld}}, \quad (2)$$

where $G_{P,ld}$, τ_{ld}, ω_{ld}, a_I, and τ_I are the lead compensator gain, the time constant, the frequency of the maximum phase lift, the integral term gain scale coefficient, and the integral time constant, respectively.

Following [1], we modify this controller into the cascaded PI/PD structure with the transfer function (1) for $a_I = 0$ in the inner control loop. In the outer control loop we apply the PI controller term with the transfer function

$$G_{pi}(s) = G_{P,pi}\left(\frac{\tau_I s + a_P}{\tau_I s}\right), \quad (3)$$

where a_P and $G_{P,pi}$ are the proportional term gain coefficient and the overall PI controller gain, respectively.

The reference controllers for PID and PI/PD are hand tuned according to rules suggested in [1].

LQ and LQ/LTR control

For LQ control the accuracy of the plant model is crucial. The control designs of the LQ regulator (LQR) with the Kalman filter and the LQ / loop transfer recovery (LTR) controllers are based on a detailed coupled, MIMO plant model obtained using FEM. The actuator dynamics are approximated with the first order model and included for each input channel in the overall plant model. The first three critical speeds of the

rotor are 260, 539, and 952 Hz. The radial suspension with four inputs, four outputs, and active control of the first flexible eigenmode is considered.

The LQR and state estimator with additional constant disturbance observer are built as presented in [5]. The estimator is formed as

$$\begin{bmatrix} \dot{\overline{\mathbf{x}}} \\ \dot{\overline{\mathbf{w}}} \end{bmatrix} = \begin{bmatrix} A & BC_w \\ 0 & A_w \end{bmatrix}\begin{bmatrix} \overline{\mathbf{x}} \\ \overline{\mathbf{w}} \end{bmatrix} + \begin{bmatrix} B \\ 0 \end{bmatrix}\mathbf{u} + L(\mathbf{y} - \overline{\mathbf{y}}), \quad (4)$$

where A, B, $\mathbf{u}$, $\mathbf{y}$, $\overline{\mathbf{x}}$, $\overline{\mathbf{y}}$, $\overline{\mathbf{w}}$, and L are the state matrix, the input matrix, the input vector, the output vector, the estimate of the state vector, the estimate of the output vector, the estimate of the disturbance signal, and the estimator gain matrix that provides satisfactory dynamics of estimation error, respectively. In the implementation $A_w=0$. However, in the design, we introduce the first order dynamics into the disturbance model to obtain a required integration time constant. The state matrix of disturbance model A_w is diagonal with the elements roughly equal to the selected inverted integrator time constant. The output matrix of disturbance model C_w is unitary. The estimator gain matrix is obtained from the steady-state solution of the Riccati equation. The computation is based on the output (sensors) noise intensity matrix R_v and the process input noise intensity matrix R_w. The state-feedback is formed by applying the feedback gain matrix K as

$$\mathbf{u} = -K\overline{\mathbf{x}} - \overline{\mathbf{w}}. \quad (5)$$

The state-feedback controller gain matrix K minimizes the quadratic integral performance index J_q, that is

$$J_q = \int_0^\infty \left[\mathbf{x}^T Q\mathbf{x} + \mathbf{u}^T R\mathbf{u}\right]dt, \quad (6)$$

where Q, R, $\mathbf{x}$, and t are the state weighting matrix, the control weight matrix, the state vector, and time. The noise covariance matrices R_v and R_w are assumed to be diagonal and are used as design parameters. For determining the diagonal weighting matrices Q and R, in the reference design, where $Q = Q_1$, we utilize the Bryson's rules [6]. The diagonal elements of Q_1 are equal to the inverse of the square of the maximum allowed values of the corresponding states. The diagonal elements of R are equal to the inverse of the squares of the maximum allowed values of the corresponding control inputs. Therefore, the reference controller for the LQ and LQ/LTR controllers is based on the diagonal weighting matrices, which are unity matrices when in per-unit quantities. According to [6], in the control layout, the state command reference input structure is utilized. The suitable reference matrices are computed from the zero steady-state error requirement of the system.

For the LQR with the Kalman filter it is difficult to achieve satisfactory robustness properties at the inputs and outputs of the plant [7]. However, for the minimum-

phase plants, the LTR procedures, which originate from [8], alleviate the controller design. Unfortunately, the LTR method, which utilizes high recovery gain, decreases the tolerable disturbance signals at high frequencies and causes problems with unmodeled dynamics. Therefore, the compromise between performance and robustness at different frequencies limits the control design. Bearing this in mind, the filter loop recovery controller is computed, by designing the controller gain matrix K that minimizes J_q in (6) with

$$Q = Q_1 + \rho C^T C, \tag{7}$$

where ρ and C are the recovery gain and the output matrix in the state-space representation. Figure 1 presents the singular value plots of the output sensitivity function for the different recovery gains, when carrying out the design in physical quantities. The gain $\rho = 1e7$ is selected because the sensitivity to unmodeled dynamics and the oscillations in time responses are anticipated.

In the design procedure of the tested and compared controllers, a genetic algorithm (GA) is used for the selection of proper control parameters. This GA provides unbiased by human error and optimized tuning of the parameters of the reference designs. The equivalent program, with the same objective function, population size, number of iterations, and genetic operations, is utilized for all investigated controllers.

Design objectives and performance indices
In the design and later in the comparison we utilize two major indices. The first is an output sensitivity function as suggested in [9] and the second is a minimum tolerated disturbance force over the frequency. When considering the MIMO systems, it is not possible to determine unequivocal Bode plots of the sensitivity and tolerated disturbance force. Therefore, the magnitudes of the singular values are used instead. The minimum singular value $\underline{\sigma}(G)$ and the maximum singular value $\overline{\sigma}(G)$ of matrix G are equal to the largest and the smallest gain for any input direction, respectively.

The output sensitivity function (i.e. a ratio of the error signal to the reference) contributes to the attenuation of the disturbance signal introduced at the position sensors. Its maximum value is used as an index representing the relative stability of a system (see e.g. [9]). The output sensitivity function is

$$S_o = \left(I + G_{pl}G_c\right)^{-1}, \tag{8}$$

where G_{pl} and G_c are the transfer function matrix of a plant and controller (feedback path), respectively. In particular, we use the peak of the maximum singular value of the frequency response for sensitivity

$$M_S = \max_{\omega} \overline{\sigma}(S_o) \tag{9}$$

that, in general, should be small for robustness.
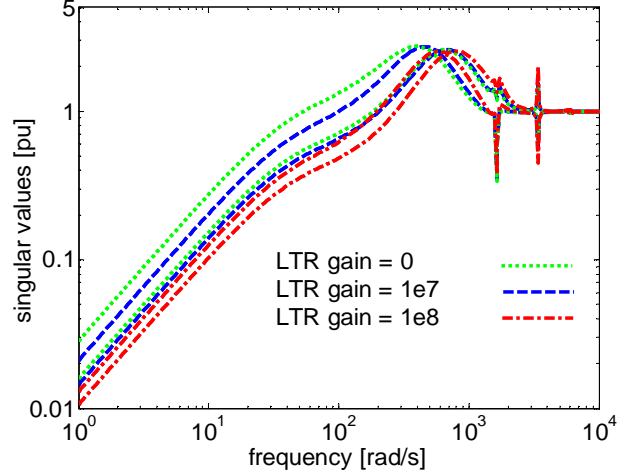
FIGURE 1: Output sensitivity (LTR controller)

The minimum tolerated disturbance force, for given frequency, is the minimum of the singular-value plots of the inverted input complementary sensitivity (i.e. an inverted ratio of the control effort to the input disturbance) and the singular value plots of the inverted input disturbance attenuation (i.e. an inverted ratio of the measured position to the input disturbance) of the MIMO radial suspension at that frequency. The input complementary sensitivity is

$$T_i = G_c G_{pl}\left(I + G_c G_{pl}\right)^{-1}. \tag{10}$$

The input disturbance attenuation is

$$T_i' = G_{pl}\left(I + G_c G_{pl}\right)^{-1}. \tag{11}$$

In the design, we evaluate the minimum tolerated disturbance force, at the frequency ω, such as

$$M_T(\omega) = \min(\underline{\sigma}(1/T_i(\omega)), \underline{\sigma}(1/T_i'(\omega))) \tag{12}$$

that, in general, should be large for disturbance rejection. Additionally, we study the peak of the minimum tolerated disturbance force M_T for all frequencies.

The singular-value plots are considered for the per-unit system. The base value of the displacement of the rotor from the central position is 300 μm; and the base value of the magnetic force is 2010 N.

Genetic algorithm for parameter optimization
Meng and Song [10] have demonstrated that the use of a fast genetic algorithm can improve the performance of the PID control. In this paper we generalize this approach to the PI/PD, LQR with the Kalman filter, and LQ/LTR controllers.

We start with defining the chromosomes. The design parameters for LQ control are the diagonal elements in the matrices Q, R, R_v, and R_w. For the LQ control, we select the six elements to be included into the chromosome. For the PID and PI/PD based control, we select the six and seven parameters to be included

into the chromosome, respectively. For the decentralized controllers, the gains $G_{P,ld}$ and $G_{P,pi}$ are considered separately for each radial bearing.

Next, we create the initial population of individual designs, which are based on the hand tuned reference controllers. We select the constant population equal to 60 individuals.

After that, the objective function (fitness function) that maps the chromosomes into fitness values is defined. These values measure the quality of the individual design in terms of the optimal solution. The objective function minimizes the sensitivity peak and maximizes the tolerated disturbance forces. Two cases are considered. The controllers are tuned in such a way that the closed-loop systems result in the same minimum tolerated disturbance forces at 180Hz and 10Hz for the case 1 and 2, respectively. The objective function is

$$J = \frac{M_{S,ref}}{M_S} + \frac{M_T}{M_{T,ref}} - 2\left|M_T(\omega) - M_{T,ref}(\omega)\right| \qquad (13)$$
$$+ \frac{M_T(\omega_1)}{10} + \frac{M_T(\omega_2)}{100},$$

where $M_{S,ref}$ and $M_{T,ref}$ are the peak sensitivity of the reference design and the minimum tolerated disturbance force of the reference design, respectively. The indices $M_T(\omega)$, $M_{T,ref}(\omega)$, $M_T(\omega_1)$, and $M_T(\omega_2)$ are evaluated at specific frequencies $\omega = 180 \cdot 2\pi$ (for the case 1), $\omega = 10 \cdot 2\pi$ (for the case 2), $\omega_1 = 260 \cdot 2\pi$, and $\omega_2 = 539 \cdot 2\pi$. The optimization is performed on the linearized plant model.

In each iteration, the new population is created in such a way that the opportunity of reproduction of each individual (selection of the individual for mating) increases with the increase of the individual fitness value. The mating is carried out by the means of mutation, crossover, and average in the corresponding entries of parents' chromosomes.

With this algorithm, two problems were observed. First, the procedure was sensitive to local minima. This was counteracted by frequent and strong mutations. Second, the single performance index could overwhelm the individual fitness value. Therefore, the individual designs are constrained so that all their performance indices have to be better than the indices of corresponding reference designs.

The convergence of the GA for the case 1 and 2 is shown in Fig. 2 and 3, respectively.

COMPARISON OF CONTROL DESIGNS

For comparison, the obtained maximum and minimum singular values of the output sensitivity and the tolerated disturbances of the closed-loop control system for the different controllers (A: PID, B: PI/PD, C: LQ, and D: LQ/LTR) and different design cases (reference, case 1, case 2) are presented in Figs. 4-8. The controllers C and D have the same reference design described earlier. The frequencies were the closed-loop systems are required to have the similar performance are shown as black solid lines for the case 1 and 2 in Figs. 5-8. Additionally, the peak output sensitivity (a: sensitivity in pu), tolerated disturbance (b: at the worst case frequency), responses to the 0.33 pu step change of the rotor position reference (c: overshoot, d: peak current) and the 0.1 pu step control current disturbance (e: displacement, f: peak current) are shown in Table 1. The peak output sensitivity is computed analytically (a1), obtained from the simulation (a2), and measured (a3). The values listed in Table 1, in columns b-f are obtained from the simulation. The simulated and measured system responses to the step change of the rotor position reference and the step change of the control current disturbance, for the controllers A-D in the case 1 and in the case 2, are presented in Figs. 9-16.

In order to approximate the sensitivity peaks, a sinusoidal position reference signal of the magnitude 0.01 pu and frequency sweep from 30 Hz to 600 Hz over a period of 9 s was applied, to one radial actuator at a time. The maximum peak obtained from the measurements, which are carried out for two radial bearings, is stored in the table. In the same manner the sensitivity peaks are determined from the experiment and from the simulations. For simulations, the method results in smaller peak values than the peak singular values obtained analytically or the peak values obtained by experiment. The analytical peak singular values correspond to the worst input directions.

TABLE 1: Comparison of the controllers

Ref	a1 (a2) a3: [pu]	b: pu	c: %	d: pu	e: pu	f: pu
A:	6.8 (3.8) --	0.15	91	0.71	0.40	0.27
B:	8.3 (4.4) --	0.13	0	0.12	0.30	0.26
C:	2.7 (2.1) --	0.37	2	0.27	0.50	0.28
case 1						
A:	5.3 (3.4) 3.6	0.18	83	0.95	0.37	0.26
B:	8.3 (4.4) 5.5	0.13	0	0.12	0.30	0.26
C:	1.9 (1.8) 2.1	0.39	2	0.12	0.69	0.28
D:	2.0 (1.8) 2.2	0.41	3	0.12	0.64	0.28
case 2						
A:	3.6 (2.2) 2.9	0.26	61	1.00	0.28	0.24
B:	8.3 (4.4) 5.5	0.13	0	0.12	0.30	0.26
C:	2.3 (2.2) 3.9	0.50	1	0.30	0.25	0.26
D:	2.3 (2.0) 2.6	0.48	1	0.21	0.32	0.25
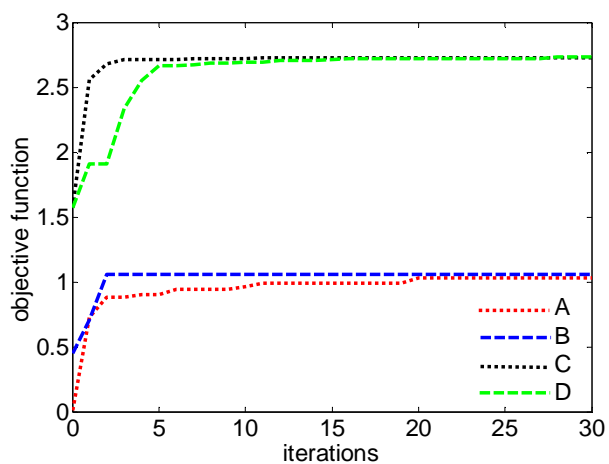
FIGURE 2: Convergence of GA (case 1)
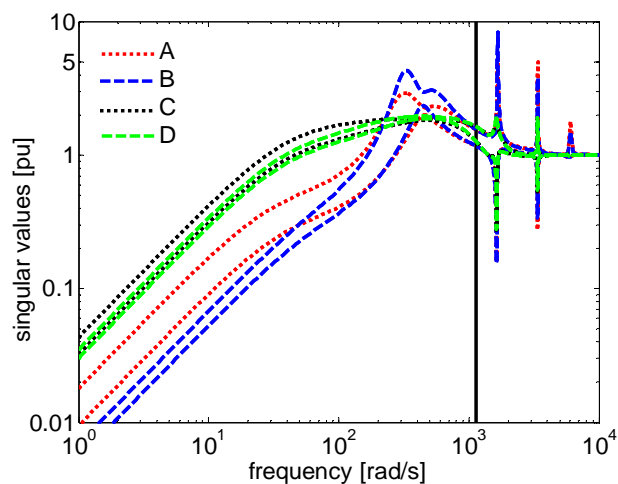
FIGURE 5: Output sensitivity (design case 1)
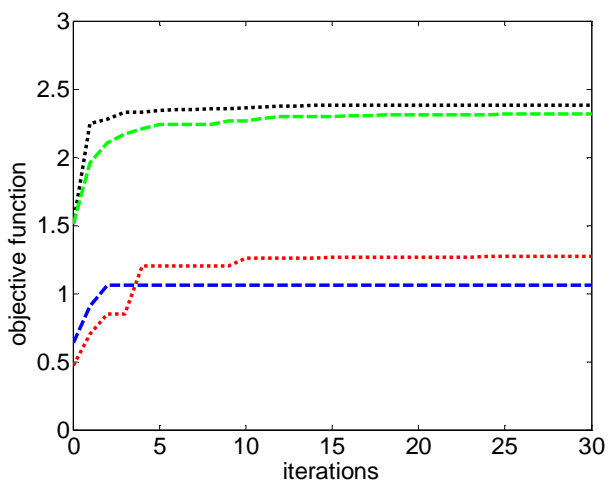
FIGURE 3: Convergence of GA (case 2)
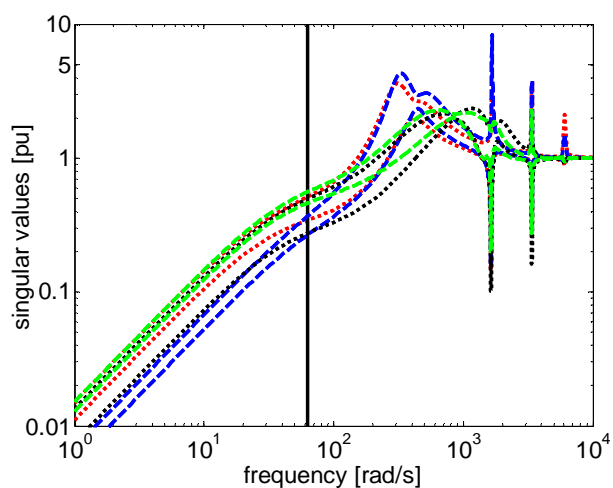
FIGURE 6: Output sensitivity (design case 2)
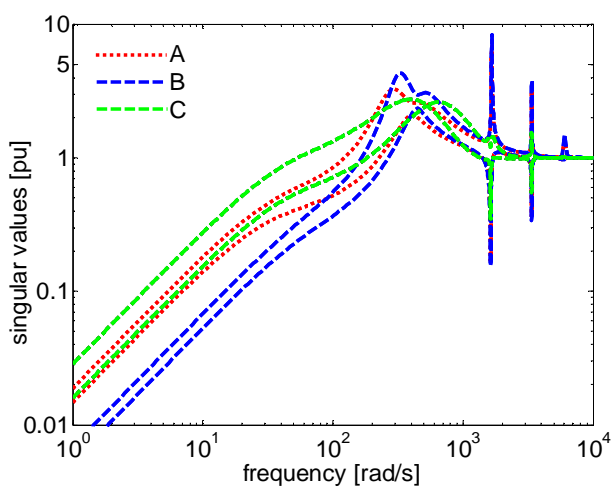
FIGURE 4: Output sensitivity (reference controllers)

similar performance
at selected frequency
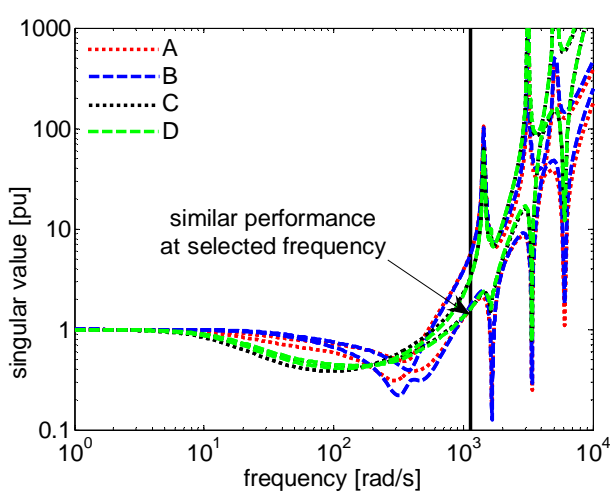
FIGURE 7: Tolerated disturbance (design case 1)
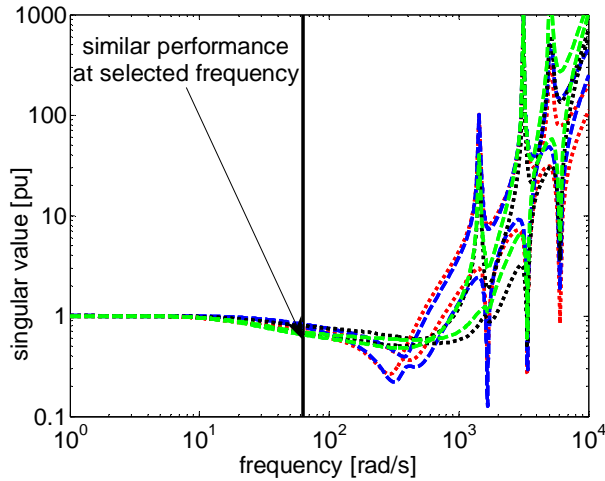
FIGURE 8: Tolerated disturbance (design case 2)

The signal sweep method results in approximated peak magnitude values because of transient system responses. However, the correspondence between the peak maximum sensitivity values, which are obtained analytically, experimentally, and by simulation, is satisfactory.

The simulation model of the AMB rotor system, which was utilized in the comparison, comprised the nonlinear actuator (as presented in [5]) and the FEM based rotor model. The modeled nonlinearities included the voltage saturation, the current saturation, the dynamic inductance and the force-field relation obtained with the reluctance network method (RNM) presented in [11]. The solution region of the RNM, was two-dimensional and it took into account the magnetic saturation, the pole cross coupling and the leakage flux over the stator slots.

Looking at the sensitivity and disturbance plots, it is apparent that the model-based optimal control methods perform significantly better at the critical speeds; also the peak sensitivity is smaller and the maximum tolerated disturbance is greater than for the decentralized controllers.

In the case 1, for the controllers A and B the feedback effectiveness at lower frequencies is better than for the controllers C and D, that is, the singular values of the PID based control sensitivity plots are lower. This results from the higher feedback gains at frequencies before the crossover; and it affects the disturbance step responses of the controllers.

In the case 2, the controllers A and B do not differ significantly when compared to the case 1. In fact, the controller B has the same performance indices for all the design cases. The limiting factors are the poor attenuation of the disturbances at the critical speeds. The controllers C and D have noticeably the higher open-loop gains than in the case 1, but they have

slightly higher maximum sensitivity peaks and the decreased performance at higher frequencies.

The described strengths and weaknesses of the controllers C and D in both design cases result from the presence of the Kalman filter.

The key point in the design is the proper formulation of the objective function and the computation of the individual fitting values. In both design cases, the controllers A and B, which are tuned with the help of the GA, are similar. The first difference between the two designs is the superior response to the step reference position of B due to the de facto two degrees of freedom controller. The second difference is the greater sensitivity of B to the high frequency flexible modes. Even greater resemblance appears between the controllers C and D in the design case 1. In the case 2, the singular value plots for C and D are slightly different. However, the performance indices are similar.
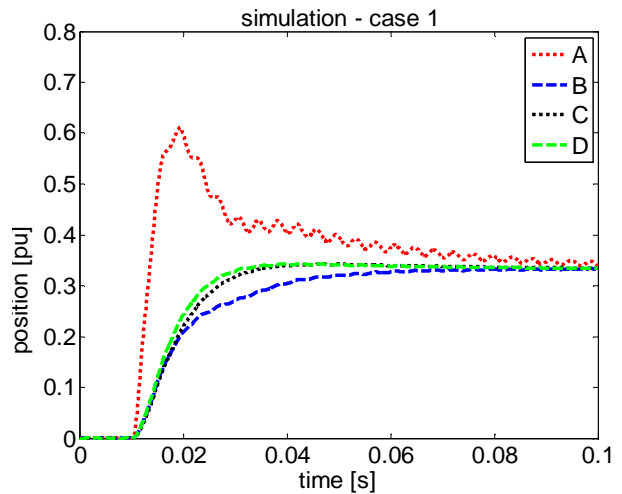
FIGURE 9: Responses to the step reference position
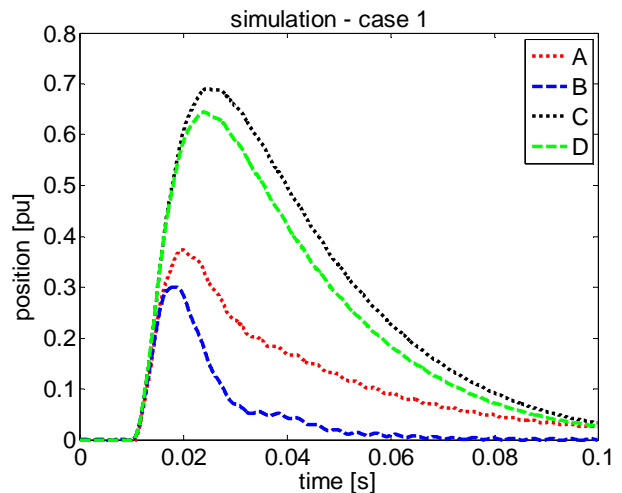
FIGURE 10: Responses to the step disturbance
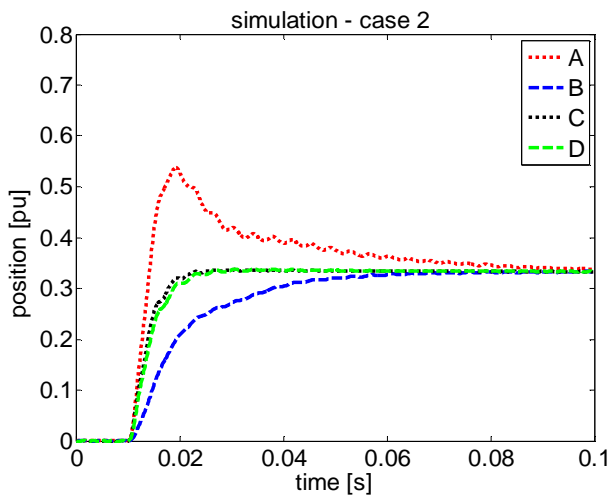
FIGURE 11: Responses to the step reference position
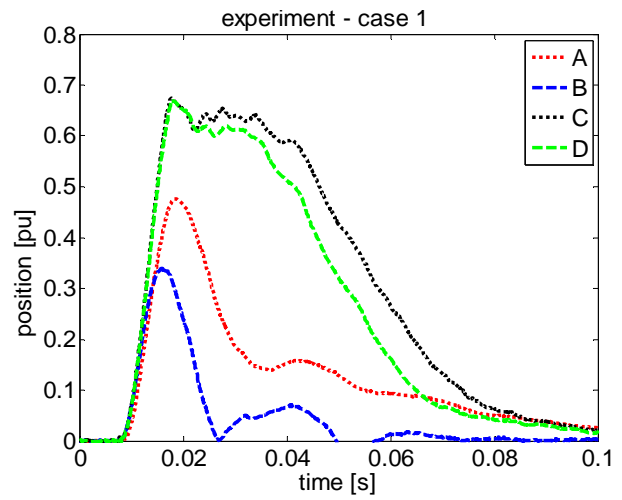
FIGURE 14: Responses to the step disturbance
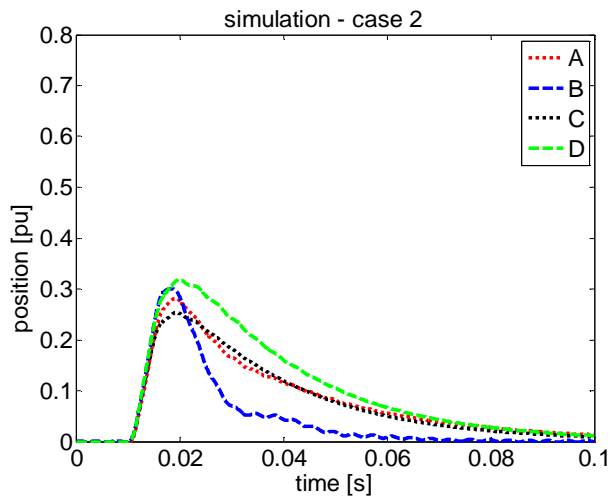
FIGURE 12: Responses to the step disturbance
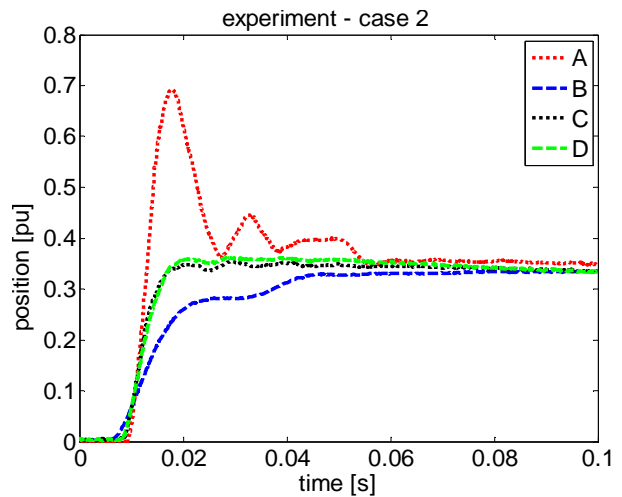
FIGURE 15: Responses to the step reference position
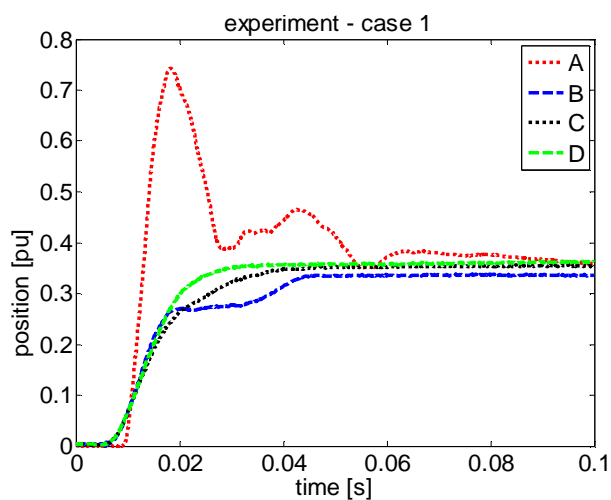
FIGURE 13: Responses to the step reference position
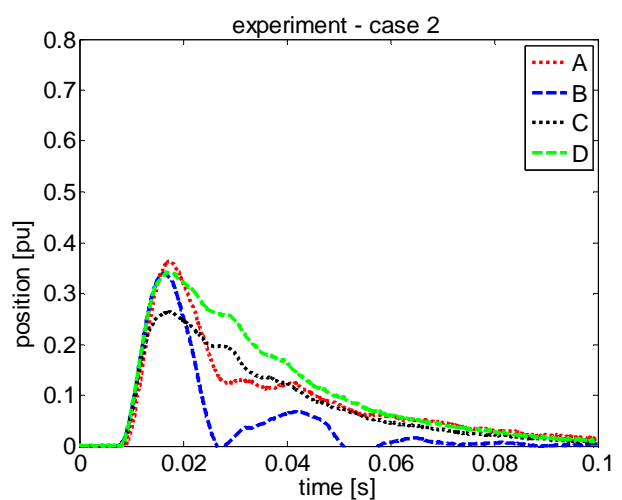
FIGURE 16: Responses to the step disturbance

CONCLUSIONS

The paper applies the genetic algorithm to evaluate the design tradeoffs of LQ, LQ/LTR, PID, and PI/PD controllers in the MIMO AMB system. The practical and credible comparison of controllers by using frequency response methods is presented.

In conclusion, the use of PI/PD and LTR ease the hand tuning of the controllers. However, when the GA and the objective tuning are utilized, the similar results can be also achieved by the classical PID and LQ control methods. The LTR provides another degree of freedom in the LQ control design; it helps in achieving a good compromise between performances at high and low frequencies, with the selection of the one parameter only, that is, the recovery gain.

For all the studied cases, the model based controllers performed better when compared to the PID based solutions. Nevertheless, the computational burden of these controllers was considerable. The digital model-based controllers were implemented as a state-space form with twenty states. As a comparison, the decentralized lead compensator required only eight states. The sampling time was 100 μs.

The genetic algorithm improved the performance and stability indices of the each tested control design when compared to the reference ones.

The controllers with the simple decentralized structure occurred to be less liable to tuning with respect to the trade offs at higher and lower frequencies, than the model based controllers. For PID and PI/PD controllers, the design trade-offs are not possible without decreasing the stability indices because of the flexible modes.

The future outlook could focus on the following aspects:

- developing the genetic algorithm, for example, using more complex multiobjective fitness function, variable population size, and variable controller order and structure, selection of individuals to retain solutions of local minima and diversity of population
- including more control methods in the comparison
- utilizing the identified plant model instead of the FEM based model
- introducing uncertainties to the plant model

References

[1] B. Polajzer, J. Ritonja, G. Stumberger, D. Dolinar, and J.-P. Lecointe, "Decentralized PI/PD position control for active magnetic bearings", Electrical Engineering 89 (1): 53-59, 2006.

[2] P. Schroder, A.J. Chipperfield, P.J. Fleming, N. Grum, "Multi-objective optimisation of distributed active magnetic bearing controllers", in IEE Proceedings of the 2nd International Conference on Genetic Algorithms in Engineering Systems: Innovations and Applications, pp. 13-18, 1997.

[3] P. Schroder, B. Green, N. Grum, P.J. Fleming, "On-line Genetic Auto-Tuning of Mixed H_2/H_∞ Optimal Magnetic Bearing Controllers", in IEE Proceedings of the International Conference on CONTROL, pp. 1123-1128, 1998.

[4] Y.N. Zhuravlyov, "On LQ-Control of Magnetic Bearing", IEEE Transactions on Control Systems Technology 8 (2): 344-350, 2000.

[5] R. Jastrzębski, Design and Implementation of FPGA-based LQ Control of Active Magnetic Bearings, Dissertation, Lappeenranta University of Technology, Finland, 2007, available:

http://urn.fi/URN:ISBN:978-952-214-509-3.

[6] G. F. Franklin, J. D. Powell, and M. Workman, Digital Control of Dynamic Systems, 3rd ed., Addison Wesley, 1998.

[7] S. Skogestad, I. Postlethwaite, Multivariable Feedback Control, 2nd ed., England: John Wiley & Sons Ltd, 2007.

[8] H. Kwakernaak, "Optimal low-sensitivity linear feedback systems", Automatica 5 (3): 279-285, 1969.

[9] H. Fujiwara, O. Matsushita, M. Ito, Y. Fukushima, "An Evaluation of Stability Indices Using Sensitivity Functions for Active Magnetic Bearing Supported High-Speed Rotor", Transactions of the ASME, Journal of Vibration and Acoustics 192: 230-238, 2007.

[10] Xiangzhong Meng, Baoye Song, "Fast Genetic Algorithms Used for PID Parameter Optimization", in IEEE Proceedings of the International Conference on Automation and Logistics, pp. 2144-2148, China, 2007.

[11] J. Nerg, R. Pöllänen, and J. Pyrhönen, "Modelling the Force versus Current Characteristics, Linearized Parameters and Dynamic Inductance of Radial Active Magnetic Bearings Using Different Numerical Calculation Methods", WSEAS Transactions on Circuits and Systems 4 (6): 551-559, 2005.